

# DEVELOPMENT OF FRAGILITY CURVES FOR REINFORCED CONCRETE BUILDINGS

Esma Souki<sup>1,2\*</sup>, Kamel Abdou<sup>1,2</sup>, Youcef Mehani<sup>3</sup>

<sup>1</sup>Department of Civil Engineering, Faculty of Sciences of Technology, Mentouri Brothers University (Constantine 1), Constantine, 25000, Algeria

<sup>2</sup>Laboratory of Materials and Construction Durability, Mentouri Brothers University (Constantine 1), Constantine, Algeria

<sup>3</sup>Department of Civil Engineering, National Earthquake Engineering Research Center CGS, Algiers, Algeria

\*Corresponding author's e-mail: asma.souki@doc.umc.edu.dz

## Abstract

**Introduction:** Algeria has experienced numerous destructive earthquakes, resulting in significant loss of human lives, buildings, and equipment. To mitigate this risk, **this study aims** to quantify the potential damage to existing strategic buildings in the city of Constantine, located in the northeast of Algeria. Many of these buildings are old, designed and constructed during the colonial era before the implementation of the Algerian seismic code. Thus, they are required to be strengthened and retrofitted. **Methods:** The LM2 method, defined in RISK-UE (WP4), based on nonlinear static analysis and spectral response, is used to develop fragility curves. In this context, a structural system mainly consists of moment-resisting reinforced concrete frames with partial infill walls. In this study, three types of strategic buildings are considered: low-rise (two stories), mid-rise (four stories), and high-rise (six stories). The current Algerian seismic code RPA99/ version 2003 (MHUV 2003) is used to assess the seismic demand. **As a result**, capacity curves are developed for two primary directions: local and global behavior, identified according to the limits specified in FEMA 356/273 and ATC 40. Based on these results, fragility curves are generated, defining four damage states: slight, moderate, extensive, and complete in terms of spectral displacement.

**Keywords:** fragility curves; damage states; LM2 method; nonlinear static analysis; RC building.

## Introduction

Assessing the seismic vulnerability of existing buildings is a very important field. This issue affects almost all buildings in Algeria, mainly because they were constructed during a period when structures were designed without seismic standards, taking into account only the impact of vertical loads. Furthermore, changes in activity, unregulated transformations, lack of maintenance, and deterioration due to budget cuts predictably can lead to safety issues in future. Fragility curves are a very useful tool for mitigating seismic risk. As a result, defining the response of these structures to earthquakes is highly complex and depends on several parameters related to the building's characteristics and seismic excitation. In Algeria, the current level of knowledge regarding the seismic behavior of buildings is not highly advanced. In this context, our investigation will focus on developing a methodology to predict damage, as expressed by fragility curves, in order to quantify potential damage that is reached or exceeded. In the field of structural earthquake engineering, fragility functions can be used to estimate the probability of occurrence of various damage states in certain buildings at an observed value of a specified intensity measure (Folić and Čokić, 2021). Our case study is based on three models of the existing strategic constructions in the city of Constantine, which

is considered the third most important city in Algeria. The structural system most commonly used at that time mainly composed of moment-resisting reinforced concrete frames with partial infill walls. In this study, three types of strategic buildings are considered: low-rise (two stories), mid-rise (four stories), and high-rise (six stories).

Several previous studies conducted by various researchers considered the important role of fragility curves as a tool for assessing seismic vulnerability and expected damage to buildings after an earthquake. Below are citations from some of them:

In 2022, Fikri and Ingham investigated the behavior of non-ductile mid-rise masonry infill buildings in New Zealand. They used the Incremental Dynamic Analysis (IDA) method, along with the generation of fragility curves. The buildings were subjected to both mainshocks and aftershocks. Fragility curves for four damage states were determined in order to examine the failure of buildings constructed before the introduction of ductility criteria. Buildings were found to have suffered slight damage from the mainshocks and severe damage from the aftershocks (Fikri and Ingham, 2022).

In 2022, Zucconi et al. analyzed the seismic performance of a reinforced concrete building designed without any seismic criteria, characterized

by a seismically-stronger and a seismically-weaker direction, such as several existing reinforced concrete-framed structures designed for vertical load only. Bidirectional ground motions were applied to the structure. The OpenSees software was used to create a 3D model, taking into account the joint deformability of the panels, which enabled the derivation of fragility curves at various states of damage corresponding to the European earthquake standard (Zucconi et al., 2022).

In 2019, Al-Nimry conducted a study on the seismic fragility of low- and mid-rise RC infilled frame buildings of 2, 4, and 6 stories in Jordan. The buildings comprised of stone-concrete infill panels. Al-Nimry relied on expert reports and conducted pushover analyses to determine the capacity response of each modeled building. The study considered four damage states and defined corresponding thresholds (Al-Nimry, 2019).

In 2016, Vazurkar and Chaudhari developed fragility curves for three RC buildings with 3 and 4 stories. The method involved modeling the structures in SAP 2000 and using pushover analysis and then utilizing the results for plotting fragility curves, aiming to reduce seismic risk. The fragility curves were generated for four damage states considering spectral displacement (Vazurkar and Chaudhari, 2016).

In 2013, Mehani et al. aimed to develop fragility curves for existing low-rise and mid-rise RC buildings in Algeria. They used Japanese Seismic Index Methodology and characterized the observed damage states of existing buildings. The study was based on the designer’s calculation method and the seismic code applied to four categories of buildings classified according to their construction period (pre-1955, during 1956–1980, during 1981–1999, and post-1999) (Mehani and al., 2013).

The main objective of these previous studies was to evaluate the effectiveness of the LM2 method to develop fragility curves, irrespective of research diversity. The parameters taken into account included various aspects, such as the typology of case studies, site characteristics, building construction systems, construction periods, software used for modeling, and compliance with seismic codes. Additionally, the methodology was applied. Despite the differences among the issues examined, this approach aims to estimate the probability of damage states and their corresponding thresholds, whether they are high or low. Finally, these results were used as preliminary data sources to assess the seismic vulnerability of buildings.

### Basics of the LM2 method

#### Nonlinear static analysis

A building’s capacity is represented by a force-displacement model (Fig. 1). It is obtained by applying the nonlinear static method, which defines

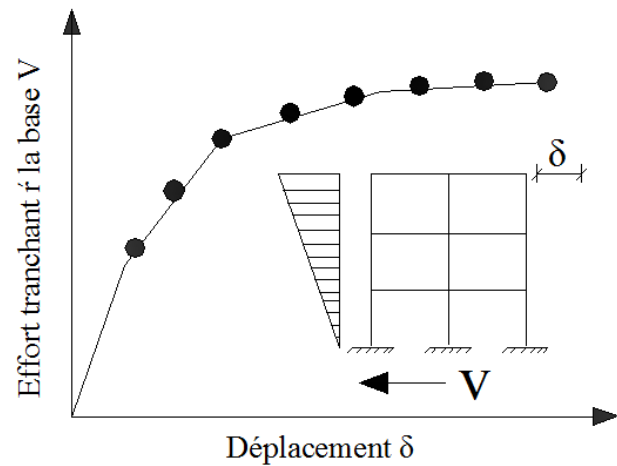


Fig. 1. The physical significance of the capacity curve defined by the base shear force as a function of displacement. (Roy and al., 2007)

the response of the structure when subjected to an increasing lateral load according to a predefined model assimilated to a system response. This response considers a single equivalent degree of freedom, driven by a single dominant vibration mode, until it reaches a target displacement (Souki and Djebbar, 2014). Additionally, it assesses the development of damage (Milutinovic and Trendafiloski, 2003). Bilinearization is used to build capacity curves, and the model is defined by control points — yield capacity and ultimate capacity in accordance with the FEMA 273 guidelines (FEMA 273, 1997).

Creating a capacity curve is the most important and challenging task, considering factors such as geometric configuration, material characteristics, type of construction system, technology used, and seismic code requirements (Milutinovic and Trendafiloski, 2003).

#### Development of fragility curves

Developing fragility curves for structures is based on analytical studies of structures. Fragility curves are derived from a resulting function identified in the damage probability matrix for buildings exceeding ( $P_{sk}[D_s > d_s | Y = y_k]$ ) or being ( $P_{sk}[D_s = d_s | Y = y_k]$ ) within a particular damage state threshold (Milutinovic and Trendafiloski, 2003). This is a function of nonlinear response, determined by spectral demand or seismic intensity (Nollet and al., 2009). Damage states can be classified into four categories: slight, moderate, extensive, and complete. It is standard practice to exclude the “D” or “No Damage” state from fragility curves (Baylon and al., 2023). A fragility curve from a model is characterized by the median value and the log-normal standard deviation ( $\beta$ ) of seismic hazard parameter, i.e., the spectral displacement  $S_d$  (Milutinovic and Trendafiloski, 2003):

$$P[d_s / S_d] = \varphi \left[ \frac{1}{d_s} \ln \left( \frac{S_d}{\bar{S}_{d,d_s}} \right) \right], \quad (1)$$

$S_{d,i}$ : is the spectral displacement (seismic hazard parameter).

$S_{d,d_s}$ : is the median value of spectral displacement at which the building reaches a certain threshold of the damage state  $d_s$  (Milutinovic and Trendafiloski, 2003).

$\beta_{d_s}$ : is the standard deviation of the natural logarithm of spectral displacement of the damage state  $d_s$ .

$\Phi$ : is the standard normal cumulative distribution function.

**Damage states**

The damage probability matrix (DPM) for systematic damage situations, derived from the harm caused by a previous earthquake or an appropriate parametric structural response, is used to study the expected likelihood of damage occurring in existing buildings. However, simplified methods were used to study the damage state thresholds ( $d_s$ ), which are determined by the capacity curves calculated from the studied structures. Based on the fragility curves, specific damage states (ds) are defined in terms of four categories: slight, moderate, extensive, and complete. The threshold value ( $\bar{S}_d$ ) and the standard deviation ( $\beta_{d_s}$ ) for each damage state can be determined using the bi-linear spectrum curve (Barbat and al., 2010; Lantada and al., 2010) (Fig. 2, Table 1), based on the threshold value of the

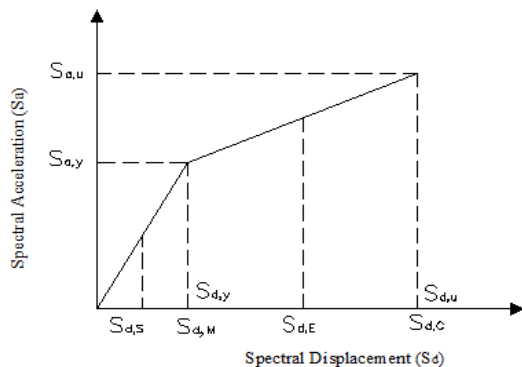


Fig. 2. Threshold values of the damage state as a function of the bilinear capacity spectrum (Nagashree and al., 2016)

damage state according to the LM2 method of RISK-UE (Milutinovic and Trendafiloski, 2003).

**Methodology guideline**

Estimating the probability of damage involves a series of steps summarized in this guideline:

1. Selecting and identifying buildings, taking into account their span and number of stories.

2. Defining the behavioral laws of materials according to the Algerian concrete standard (DTR, B., 1993), modeled as confined and unconfined concrete (Mander and al, 1988), with longitudinal and transverse steel.

3. Modeling the structure in 3D using appropriate software, considering static loading conditions including dead and live loads.

4. Defining the seismic demand according to the Algerian seismic code RPA99/version 2003 (MHUV 2003). It can be expressed by Eq. (2) below:

$$\frac{S_a}{g} = \begin{cases} 1.25A \left( 1 + \frac{T}{T_1} \left( 2.5\eta \frac{Q}{R} - 1 \right) \right) & 0 \leq T \leq T_1; \\ 2.5\eta(1.25A) \left( \frac{Q}{R} \right) & T_1 \leq T \leq T_2; \\ 2.5\eta(1.25A) \left( \frac{Q}{R} \right) \left( \frac{T_2}{T} \right)^{2/3} & T_2 \leq T \leq 3.0s; \\ 2.5\eta(1.25A) \left( \frac{T_2}{3} \right)^{2/3} \left( \frac{3}{T} \right)^{5/3} \left( \frac{Q}{R} \right) & T > 3.0s, \end{cases} \quad (2)$$

where:

A: the ground acceleration of 0.25 g. The soil is classified as a firm site (S2) according to the Algerian seismic code RPA99/version 2003 (MHUV 2003). The vibration periods corresponding to the horizontal axis as a function of spectral acceleration are  $T_1 = 0.15$  s and  $T_2 = 0.40$  s, with R representing the global behavior factor.

5. The identification of plastic hinges, as described by an idealized behavioral law and performance limits outlined in FEMA 356 (FEMA, 2000), applies to composite bending columns and simple bending beams.

Table 1. Relationship between the threshold ( $\bar{S}_d$ ) and standard deviation ( $\beta_{d_s}$ ) for each damage state

| Damage states | Median value                           | Standard deviation                |
|---------------|--|-----------------------------------|
| Slight        | $\bar{S}_{d1} = 0.7D_y$                | $S_{d1} = 0.25 + 0.07 \ln(\mu_u)$ |
| Moderate      | $\bar{S}_{d2} = D_y$                   | $S_{d2} = 0.2 + 0.18 \ln(\mu_u)$  |
| Extensive     | $\bar{S}_{d3} = D_y + 0.25(D_u - D_y)$ | $S_{d1} = 0.1 + 0.4 \ln(\mu_u)$   |
| Complete      | $\bar{S}_{d4} = D_u$                   | $S_{d1} = 0.15 + 0.5 \ln(\mu_u)$  |

Where:

$\bar{S}_d$  : is the median value of spectral displacement, and subscripts 1, 2, 3, and 4 indicate the damage state: slight, moderate, extensive, and complete, respectively.

$D_y$  : is the yield spectral displacement.

$D_u$  : is the ultimate spectral displacement.

6. The evolution of the capacity curves in the case studies (force-displacement) progresses differently along the two primary directions, XX and YY.

7. Converting the demand and capacity curves into the Acceleration Displacement Response Spectrum (ADRS) form (Hemsas and Elachachi, 2007), according to the ATC 40 guidelines (Applied Technology Council, 1996).

8. The bilinear idealization (Fig. 3) of ADRS curves is characterized by two limit states: Yield and ultimate (Milutinovic and Trendafiloski, 2003), according to the FEMA 273 guidelines (FEMA 273, 1997).

9. Overlaying two curves of capacity and demand to determine the performance point at their intersection (Fig. 4).

10. The evolution of the fragility curve is based on the shape of the log-normal probability of predicted damage in terms of spectral displacement. Damage states are categorized as slight, moderate, extensive, and complete.

11. Estimating the probabilities of damage for each potential damage state described for a given performance point according to the appropriate fragility model (Fig. 5).

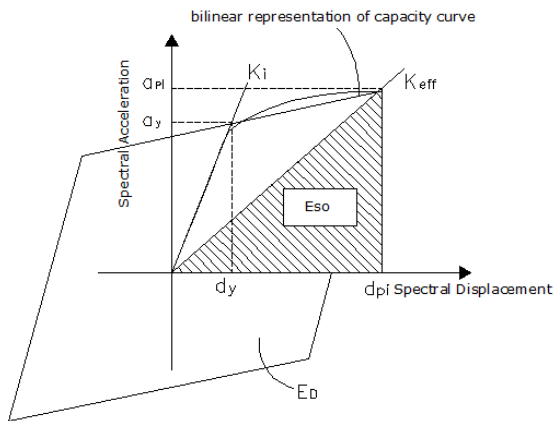


Fig. 3. Capacity curve in ADRS format (Mouroux and al., 2021)

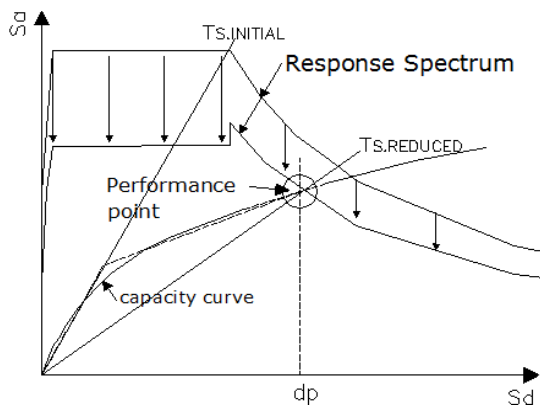


Fig. 4. Determination of the performance point (Mouroux and al, 2021)

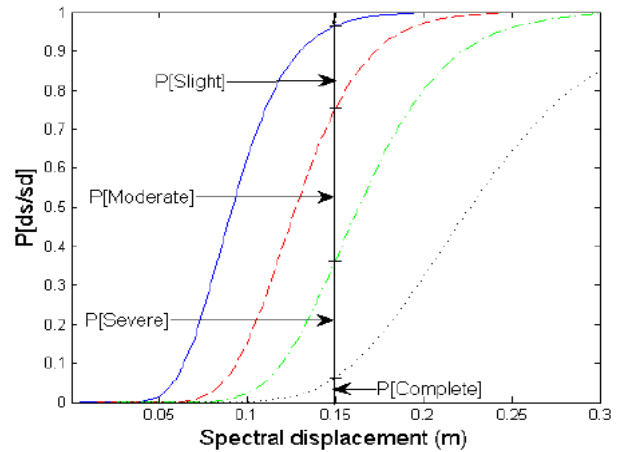


Fig. 5. Probability for each damage state as a function of spectral displacement (Barbat et al, 2012)

### Analytical modeling

This paper presents the development of fragility curves using the LM2 method described in RISK-UE (Milutinovic and Trendafiloski, 2003), using two sets of functions: capacity and building demand. The structural system of the models consists of frame-type structures with partial infill walls, applied to three types of existing strategic reinforced concrete buildings. The buildings were constructed between 1980 and 2008 in accordance with Algerian regulations and are therefore classified as having low code compliance. The models are low-, medium-, and high-rise, with 2, 4, and 6 stories, respectively. Each model is characterized by a different number of stories. The design of these buildings considering the response spectrum was numerically modeled in three dimensions using ETABS version 9.7.2 and SAP 2000 version 2014 to calculate plastic hinges. The structures were designed to withstand dead and live loads, as well as seismic forces, based on the response spectrum of zone IIa, group 1A, and design acceleration of 0.25 g in accordance with RPA99/version 2003 (MHUV 2003). The modeling of buildings depends on various parameters related to the structural design and seismic excitation, considering geometric sizes, material properties, and reinforcement of structural elements according to load guidelines (DTR, B. C. 2.2, 1988). It is worth noting that the lateral resistance systems of the three models differ: model 1 features external walls and internal partitions made of brick, model 2 incorporates filled hollow bricks in masonry, while model 3 uses external walls made of concrete blocks. The modeled structures are shown in Fig. 6.

The following Tables 2 and 3 summarize all the parameters mentioned above.

The simultaneous effects of gravity and lateral loads are typically included in the nonlinear analysis of structures (Al-Nimry, 2019). Therefore, a triangular loading model is employed to account for lateral

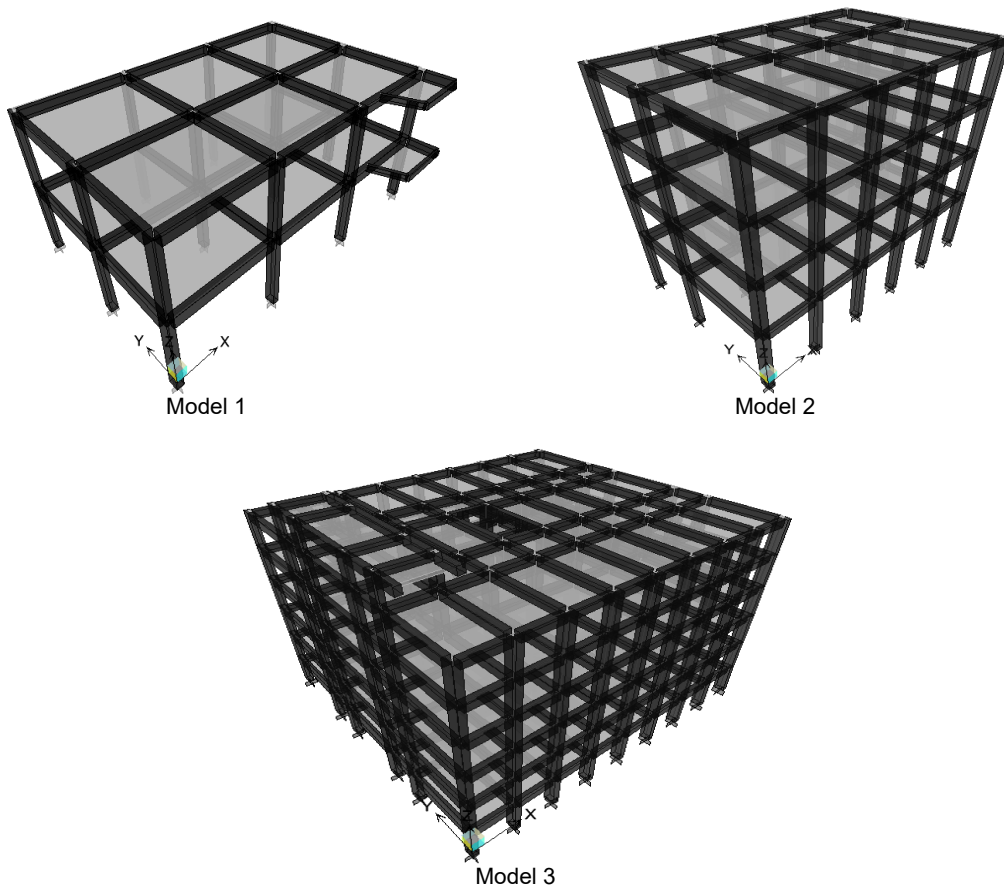


Fig. 6. Representative building structure models

Table 2. Geometric and structural characteristics of different buildings

| Model 3   | Model 2   | Model 1   | Model characteristics                                  |
|---|---|---|--|
| <b>6</b>  | <b>4</b>  | <b>2</b>  | <b>No. of stories</b>                                  |
| Story '1'<br>H = 3.45 m<br>Stories ,2, 3, 4, 5, 6'<br>H = 3.55 m  | Story '1'<br>H = 4.36 m<br>Stories ,2, 3, 4'<br>H = 3.6 m   | Stories '1, 2'<br>H = 3.5 m   | Height of stories                                      |
| Built in the 1980s  | 817.0675 m <sup>2</sup><br>Built in 2008  | 456.705 m <sup>2</sup><br>Built in 2000   | Floor area (m <sup>2</sup> )<br>Period of construction |
| Hospital administrative and medical unit<br>El Khroub   | Administrative unit of the government building, Daksi   | Surgical clinic of the children's hospital, El Mansourah  | Location   |
| Hollow concrete block, thickness: 20 + 5 cm   | Hollow concrete block, thickness: 16 + 4 cm   | Full slab, thickness: 20 cm   | Floor type   |
| Corner<br>(50x90) cm <sup>2</sup> 8φ16 + 10φ16<br>Edge<br>(35x55) cm <sup>2</sup> 8φ16 + 4φ14             | Corner<br>(35x55) cm <sup>2</sup> 8φ16 + 4φ14<br>Edge<br>(35x55) cm <sup>2</sup> 8φ16 + 4φ14<br>Center<br>(35x55) cm <sup>2</sup> 8φ16 + 4φ14                                 | Corner<br>(30x45) cm <sup>2</sup> 6φ14 + 2φ12<br>Edge<br>(30x45) cm <sup>2</sup> 6φ14 + 2φ12<br>Center<br>(30x45) cm <sup>2</sup> 6φ14 + 2φ12 | Columns<br>(dimensions, reinforcement)                 |
| Principal<br>(50x75) cm <sup>2</sup><br>8φ14 + 6φ12<br>Chainage<br>(50x75) cm <sup>2</sup><br>8φ14 + 6φ12 | Principal<br>(35x55) cm <sup>2</sup><br>6φ14 + 2φ10<br>Chainage type 1<br>(35x40) cm <sup>2</sup><br>6φ12 + 2φ10<br>Chainage type 2<br>(35x75) cm <sup>2</sup><br>6φ14 + 4φ12 | Corner (30x45) cm <sup>2</sup><br>6φ10 + 2φ12<br>Center<br>(30x45) cm <sup>2</sup><br>6φ10 + 2φ12   | Beams<br>(dimensions, reinforcement)                   |

Table 3. Characteristics of concrete and steel materials

| Steel                   | Concrete                | Characteristics of materials |
|-------------------------|-------------------------|------------------------------|
| –                       | 20 MPa                  | Compressive strength         |
| 2.1E+5 (MPa)            | 29,858.594 (MPa)        | Modulus of elasticity        |
| 0.002                   | 0.002                   | Elastic strain               |
| 0.01                    | 0.0035                  | Ultimate strain              |
| –                       | 15 cm                   | Spacing of confinement       |
| 78 (kN/m <sup>3</sup> ) | 25 (kN/m <sup>3</sup> ) | Unit weight                  |
| 400 MPa (HD)            | –                       | Yield strength               |
| 400 MPa                 | –                       | Ultimate strength            |

forces, considering (G + bQ), and an additional vertical force due to the structure’s weight defined by the combination (G + Q). The behavioral law of a plastic hinge for composite bending columns and simple bending beams is described using the Section Designer calculation of SAP 2000 software version 2014 and is idealized in two parts. The first part is limited by the initial yield, which involves the appearance of cracking in the concrete and the initial softening of the steel. The second part is limited by the point of maximum strength and deformation (Souki and djebbar, 2014). Additionally, the shear capacity of columns and beams is considered, including axial force from the vertical load, shear strength, and flexural strength, which are indicated in Eq. (3) (Waenpracha et al., 2023).

$$L_p = 0.08L_v + 0.022f_y d_{bl} \quad (3)$$

$L_v$  : shear length.

$L_p$ : plastic hinge length.

$d_{bl}$ : diameter of the longitudinal rebar.

$f_y$ : yield strength of the longitudinal rebar.

This is recorded as the extent of the plastic hinge (Park et al., 1982). It was developed based on experimental findings from specimens of reinforced

concrete with well-detailed plastic hinge regions consisting of deformed reinforcing bars (Souki and Djebbar, 2014). The details of the previously established plastic hinge law are shown in Fig. 7.

### Results and discussion

The analysis of different structures using the nonlinear static procedure, more commonly known as pushover analysis, provided us with capacity curves. These curves were obtained for the two considered directions (XX) and (YY) for each model (Fig. 8).

Following the analysis of the capacity curves beyond the elastic range and considering the development of plastic hinges from their appearance in any structural element up to a certain level of damage, their characteristics include resistance to bending and deformation capacity. They are influenced by several factors such as the intensity of the normal force, the volumetric ratio of transverse reinforcement, the longitudinal reinforcement ratio, and the material behavior laws applied. In general, their properties are determined by the nature, typology, and geometry of the structures.

The base shear capacity obtained in model 3 is twice as high as that obtained in models 1 and 2 in both directions XX and YY. However, the displacements recorded in model 1 are higher than those obtained in models 2 and 3, with variations ranging from 18 to 31 % in the YY direction and 30 % in the XX direction.

This implies that building model 3 demonstrates the greatest capacity to resist lateral loads in both directions compared to building models 1 and 2. Conversely, model 1 exhibits the lowest capacity to resist lateral loads in both directions. Additionally, it undergoes greater displacement and experiences higher energy dissipation compared to models 2 and 3. This suggests that model 3 is more rigid and resistant, whereas model 1 offers significant ductility and flexibility, enabling it to endure greater deformations before failure. Physically, these differences could be attributed to various factors

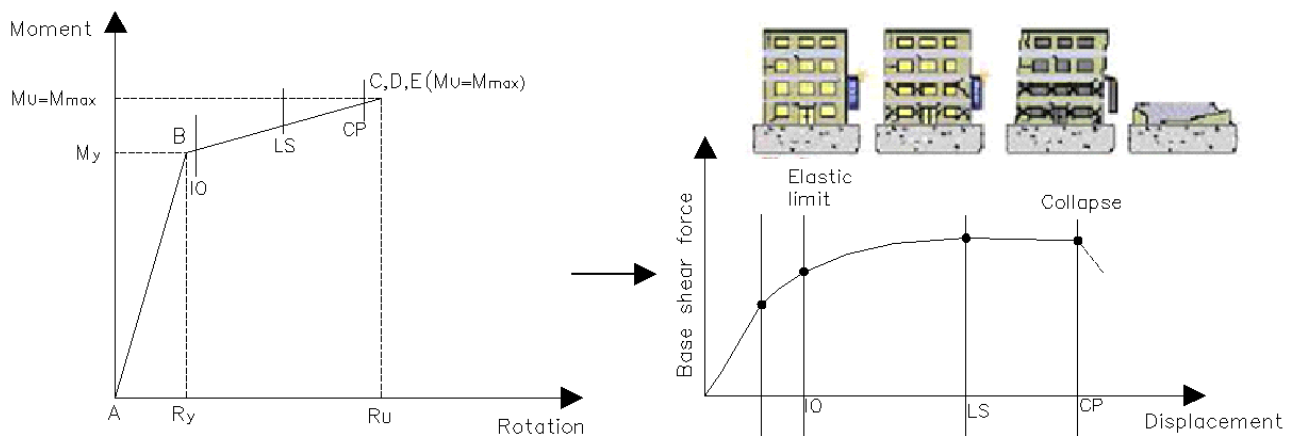


Fig. 7. Simplified plastic hinge law and capacity curve

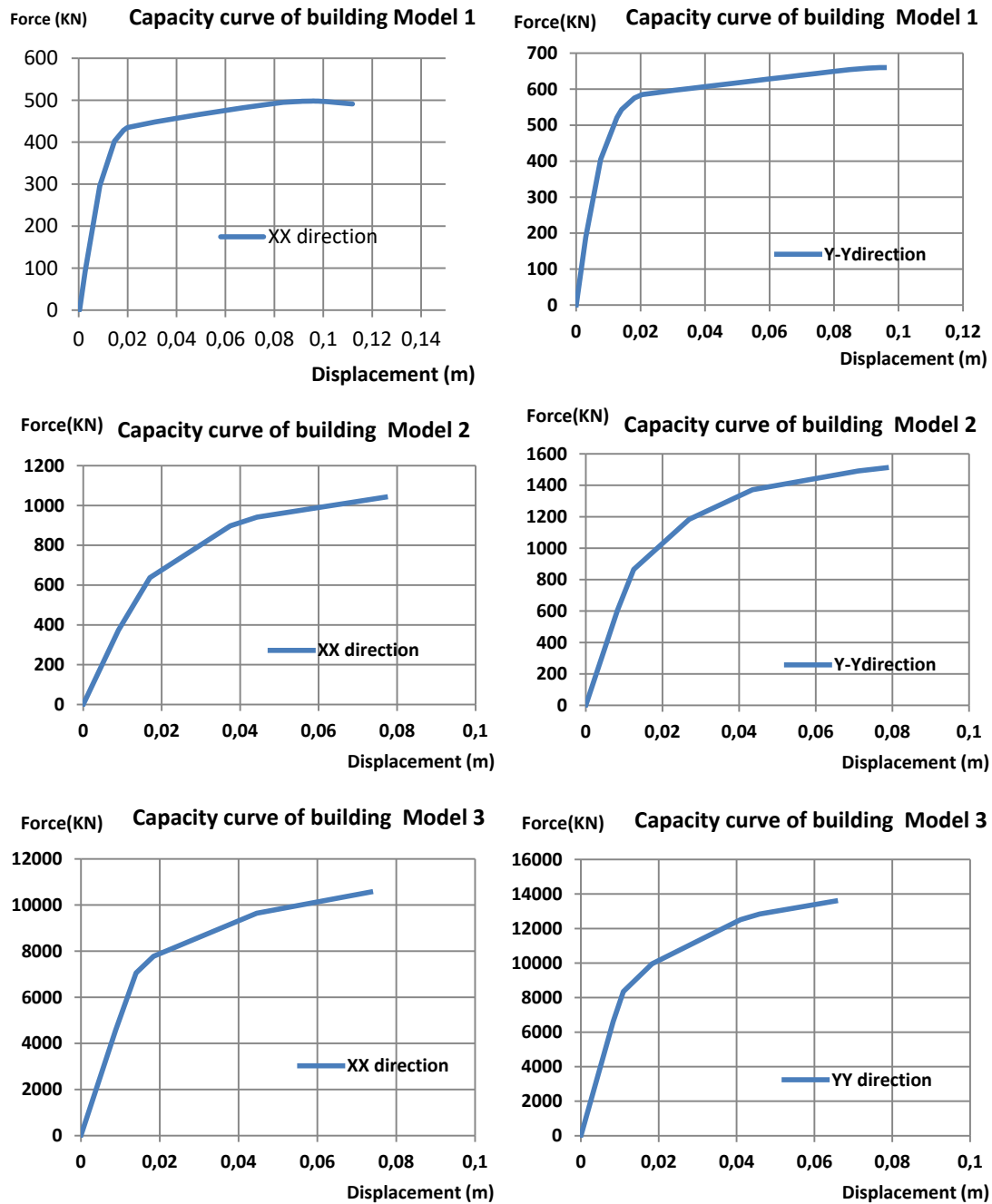


Fig. 8. Capacity curves of low-, mid- and high-rise buildings in the XX and YY directions

such as building geometry, mass distribution, and the stiffness of structural elements. Model 3 has more favorable geometry, optimized mass distribution, and stiffer structural elements, contributing to its higher capacity and lower displacement under lateral loads. Conversely, model 1 has smaller geometry, mass, and structural elements, which result in lower capacity and greater displacement under lateral loads.

The real behavior laws were converted into curves in the form of ADRS (acceleration displacement response spectrum) in accordance with the ATC-40 guide (Applied Technology Council, 1996). The curves are idealized in a bilinear form, taking into

account the limits established by the FEMA 356 guide (FEMA, 2000). Finally, the results of the two boundary states, elastic and ultimate, of spectral acceleration and displacement, as well as the mean value and standard deviation  $S_A$  and  $S_d$  of each damage state, are summarized in Table 4.

The fragility curves were determined by the log-normal standard deviation ( $\beta$ ) and the median value ( $\bar{S}_d$ ), which are influenced by spectral displacement  $S_d$  (Fig. 9).

The results indicate that incorporating three-dimensional structural modeling and considering bi-directional ground motion are fundamental aspects

Table 4. Damage states with considered yield and ultimate points

| Building models | Yield point |          | Ultimate point |          | Damage state thresholds (spectral displacement in cm) |          |                |          |                |          |                |          |
|-----------------|-------------|----------|----------------|----------|---|----------|----------------|----------|----------------|----------|----------------|----------|
|                 | SAy (%g)    | SDy (cm) | SAu (%g)       | SDu (cm) | $\bar{S}_{d1}$  | $\beta1$ | $\bar{S}_{d2}$ | $\beta2$ | $\bar{S}_{d3}$ | $\beta3$ | $\bar{S}_{d4}$ | $\beta4$ |
| Model '1' xx    | 0.12        | 1.37     | 0.13           | 4.25     | 0.95  | 0.32     | 1.37           | 0.40     | 2.09           | 0.55     | 4.25           | 0.71     |
| Model '2' xx    | 0.12        | 2.00     | 0.14           | 11.4     | 1.40  | 0.37     | 2.00           | 0.51     | 4.35           | 0.79     | 11.4           | 1.02     |
| Model '3' xx    | 0.13        | 1.16     | 0.16           | 7.89     | 0.81  | 0.38     | 1.16           | 0.54     | 2.84           | 0.86     | 7.89           | 1.10     |
| Model '1' yy    | 0.18        | 1.10     | 0.19           | 8.28     | 0.75  | 0.39     | 1.08           | 0.56     | 2.88           | 0.91     | 8.28           | 1.16     |
| Model '2' yy    | 0.15        | 4.29     | 0.16           | 9.20     | 3.00  | 0.36     | 4.29           | 0.48     | 5.51           | 0.73     | 9.20           | 0.94     |
| Model '3' yy    | 0.18        | 1.80     | 0.21           | 6.60     | 1.26  | 0.34     | 1.80           | 0.43     | 3.00           | 0.61     | 6.60           | 0.79     |

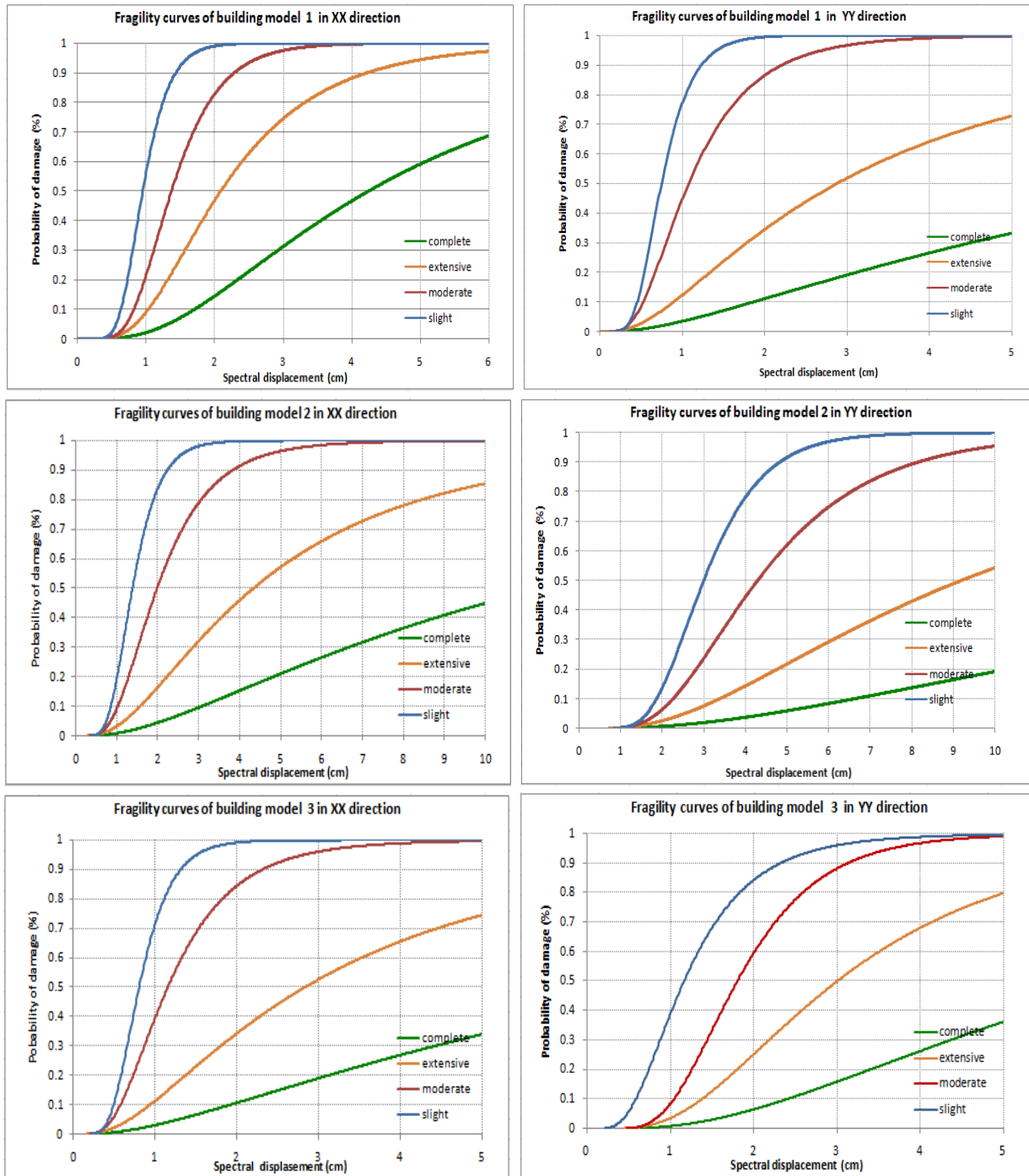


Fig. 9. Fragility curves for RC building models in the XX and YY directions



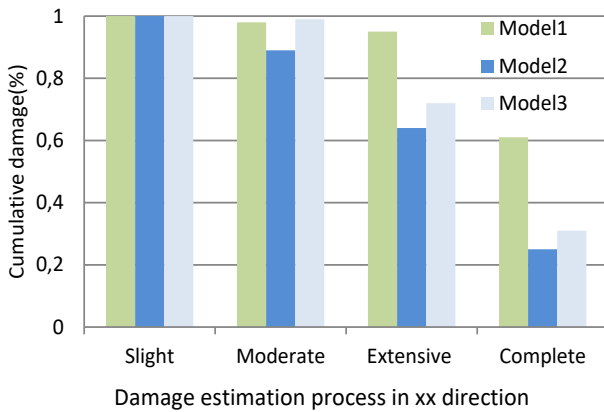


Fig. 10. Damage probability evaluation for RC building models in the XX direction

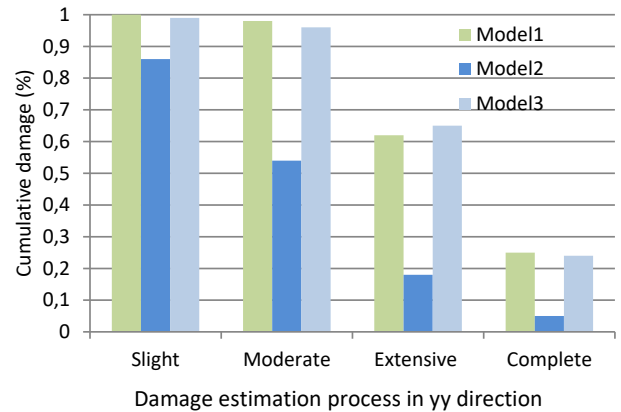


Fig. 11. Damage probability evaluation for RC building models in the YY direction

in analyzing fragility curves. Specifically, the findings highlight that fragility curves show a steeper incline for the “slight” and “moderate” damage thresholds in both the XX and YY directions across all three examined models. This suggests that models 1, 2, and 3 are more susceptible to fragility and vulnerability in both orientations. Furthermore, this structural behavior is confirmed in Table 4, which reveals that the median values of the fragility curves are consistently lower in both directions and for both damage thresholds, “slight” and “moderate”, regardless of the model under consideration. Conversely, the fragility curves for the “extensive” and “complete” damage states illustrate reduced vulnerability of the structures. This is supported by the slight upward trend observed in the fragility curves, aligning with higher median values across all three models and in both directions analyzed.

The results of the damage probability evaluation for each damage state in the XX and YY directions for the studied buildings are shown in Figs. 10 and 11, respectively.

The main objective of this study was to assess the seismic vulnerability of structures by calibrating the fragility curves using the LM2 method, as outlined in RISK-UE. Significant emphasis was placed on the structural modeling of the analyzed models, as well as on characterizing seismic inputs and identifying damage state thresholds. Ultimately, the results of the probability of damage states estimated from the analysis of the fragility curves of the examined buildings indicate higher vulnerability, primarily observed in most models for slight and moderate damage states

in both the XX and YY directions. Conversely, for extensive and complete damage states, vulnerability is comparatively lower and more restrictive, which is particularly evident in model 2 in the YY direction.

**Conclusion**

This paper discusses the application of the concepts of the LM2 method, as described in RISK-UE, for the development of fragility curves for existing strategic reinforced concrete buildings, using the nonlinear static analysis approach, which is a function of spectral displacement or seismic earthquake parameters. The pushover analysis demonstrates the true behavior of the structure and enables the estimation of various resistance and displacement characteristics. It also facilitates specifying the level of damage assessment and deducing the degree of ductility. This study contributes to assessing the seismic vulnerability of strategic buildings in major Algerian cities, focusing on Constantine, the eastern capital, with the aim of mitigating seismic risks. Furthermore, it aims to review and improve various earthquake regulations and seismic rules. The findings from the fragility curve analysis provide a broader vision and perspective for a more precise understanding of Algeria’s seismic risk. The fragility curve is considered an excellent source for preliminary seismic analysis to assess the level of seismic vulnerability, as well as for upgrading and retrofitting existing buildings in Algeria. In future research, our goal will be to study other constructions involving shear walls and dual systems.

## References

- Al-Nimry, H. (2019). Development of seismic fragility curves of RC infilled frame buildings in Jordan. *MATEC Web of Conferences*, Vol. 281, 01012. DOI: 10.1051/mateconf/201928101012.
- Applied Technology Council (1996). *ATC-40. Seismic evaluation and retrofit of concrete buildings*. Redwood City: Applied Technology Council, 346 p, California, USA.
- Barbat, A. H., Carreño, M. L., Pujades, L. G., Lantada, N., Cardona, O. D., Mabel, C., and Marulanda, M. C. (2010). Seismic vulnerability and risk evaluation methods for urban areas. A review with application to a pilot area. *Structure and Infrastructure Engineering*, Vol. 6, Issue 1–2, pp. 17–38. DOI: 10.1080/15732470802663763.
- Barbat, A. H., Vargas, Y. F., Pujades, L. G., and Hurtado, J. E. (2012). Probabilistic assessment of the seismic damage in reinforced concrete buildings. In: *Computational Civil Engineering – CCE2012. 43 International Symposium*, May 25, 2012, Iasi, Romania, pp. 43–61.
- Baylon, M. B., Sevilla, M. E. P., Cutora, M. D. L., Villa, R. M. S., Reynes, P. M. P., and Montemayor, J. M. V. (2023). Development of fragility curves for seismic vulnerability assessment: the case of Philippine General Hospital spine building. *International Research Journal of Science, Technology, Education, and Management*, Vol. 2, No. 4, pp. 1–11. DOI: 10.5281/zenodo.7559408.
- Ministry of Housing and Urbanism, M.H.U.V., and National Center of Applied Research in Earthquake Engineering, C.G.S. (2003). *Algerian Seismic Regulation, RPA 99 version 2003, D.T.R - B. C. 2.48 Algeria*.
- FEMA (1997). *NEHRP guidelines for the seismic rehabilitation of buildings. FEMA 273*. Washington, DC: FEMA, 435 p.
- FEMA (2000). *Prestandard and commentary for the seismic rehabilitation of buildings. FEMA 356*. Washington, DC: FEMA, 518 p.
- Fikri, R. and Ingham, J. (2022). Seismic response and aftershock fragility curves for non-ductile mid-rise buildings comprised of reinforced concrete frame with masonry infill. *Structures*, Vol. 45, pp. 1688–1700. DOI: 10.1016/j.istruc.2022.09.108.
- Folić, R. and Čokić, M. (2021). Fragility and vulnerability analysis of an RC building with the application of nonlinear analysis. *Buildings*, Vol. 11, Issue 9, 390. DOI: 10.3390/buildings11090390.
- DTR, B. C. 2.2 (1988). *Dead loads and live loads*. Edition of the National Center for Applied Research in Earthquake Engineering, C.G.S.
- Hemsas, M. and Elachachi, S. M. (2007). Performance evaluation and analysis of the nonlinear behavior of reinforced concrete shear walls subjected to seismic action. 25th AUGC Meeting, p. 23-25.
- Lantada, N., Irizarry, J., Barbat, A. H., Goula, X., Roca, A., Susagna, T., and Pujades, L. G. (2010). Seismic hazard and risk scenarios for Barcelona, Spain, using the Risk-UE vulnerability index method. *Bulletin of Earthquake Engineering*, Vol. 8, pp. 201–229. DOI: 10.1007/s10518-009-9148-z.
- Mander, J. B., Priestley, M. J. N., and Park, R. (1988). Theoretical stress-strain model for confined concrete. *Journal of Structural Engineering*, Vol. 114, Issue 8, pp. 1804–1826. DOI: 10.1061/(ASCE)0733-9445(1988)114:8(1804).
- Mehani, Y., Bechtoula, H., Kibboua, A., and Naili, M. (2013). Assessment of seismic fragility curves for existing RC buildings in Algiers after the 2003 Boumerdes earthquake. *Structural Engineering and Mechanics*, Vol. 46, No. 6, pp. 791–808. DOI: 10.12989/sem.2013.46.6.791.
- Milutinovic, Z. V. and Trendafiloski, G. S. (2003). RISK-UE. An advanced approach to earthquake risk scenarios with applications to different European towns. Contract: EVK4-CT-2000-00014, WP4: Vulnerability of current buildings, p. 1-111. [online] Available at: [http://www.civil.ist.utl.pt/~mlopes/conteudos/DamageStates/Risk%20UE%20WP04\\_Vulnerability.pdf](http://www.civil.ist.utl.pt/~mlopes/conteudos/DamageStates/Risk%20UE%20WP04_Vulnerability.pdf) [Date accessed: May 15, 2022].
- Mouroux, P., Negulescu, C., and Belvaux, M. (2021). Practical comparison between displacement methods, leading to performance point and ductility demand, from ATC 40 (in damping) and Eurocode 8 (in ductility). Conference paper: January 2021, pp. 2-3.
- Nagashree, B. K., Ravi Kumar, C. M., and Reddy, V. (2016). A parametric study on seismic fragility analysis of RC buildings. *Earthquakes and Structures*, Vol. 10, No. 3, pp. 629–643. DOI: 10.12989/eas.2016.10.3.629.
- Nollet, M.-J., Karbassi, A., Lefebvre, K., and Chaallal, O. (2009). Development of fragility curves for existing buildings using the applied element method. 9th National Symposium on Structural Calculation. Giens, France, paper A3H91805.
- Park, R., Priestley, M. J. N., and Gill, W. D. (1982). Ductility of square-confined concrete columns. *Journal of the Structural Division*, Vol. 108, Issue 4, pp. 929–950. DOI: 10.1061/JSDEAG.0005933.
- DTR, B. (1993). *BC 2-41: Design and calculation rule for Reinforced Concrete Structures „CBA 93”*. Edition of the National Center for Applied Research in Earthquake Engineering, C.G.S. Approved by ministerial decree of, 165-167.
- Roy, N., Paultre, P., and Proulx, J. (2007). *Seismic evaluation and rehabilitation of reinforced concrete viaduct columns*. Seismic Engineering and Structural Dynamics Research Center (CRGP). Sherbrooke University, Montreal.

- Souki, A., Djebbar, N. (2014). Influence of confinement reinforcement on the seismic performance of reinforced concrete columns. University of Constantine 1, Algeria.
- Vazurkar, U. Y. and Chaudhari, D. J. (2016). Development of fragility curves for RC buildings. *International Journal of Engineering Research*, Vol. 5, Issue Special 3, pp. 591–594. DOI: 10.17950/ijer/v5i3/016.
- Waenpracha, S., Foytong, P., Suppasri, A., Tirapat, S., Thanasisathit, N., Maneekul, P., and Ornthammarath, T. (2023). Development of fragility curves for reinforced-concrete building with masonry infilled wall under tsunami. *Advances in Civil Engineering*, Vol. 2023, 8021378. DOI: 10.1155/2023/8021378.
- Zucconi, M., Bovo, M., and Ferracuti, B. (2022). Fragility curves of existing RC buildings accounting for bidirectional ground motion. *Buildings*, Vol. 12, Issue 7, 872. DOI: 10.3390/buildings 12070872.

## ПОСТРОЕНИЕ КРИВЫХ ХРУПКОСТИ ДЛЯ ЖЕЛЕЗОБЕТОННЫХ ЗДАНИЙ

Эсма Суки<sup>1,2</sup>, Камель Абду<sup>1,2</sup>, Юсеф Механи<sup>3</sup>

<sup>1</sup>Кафедра гражданского строительства, факультет технологических наук, Университет братьев Ментури (Константина 1), Константина, 25000, Алжир

<sup>2</sup>Лаборатория материалов и долговечности конструкций, Университет братьев Ментури (Константина 1), Константина, 25000, Алжир

<sup>3</sup>Отдел гражданского строительства, Национальный исследовательский центр сейсмостойкого строительства CGS, Алжир, Алжир

\*E-mail: asma.souki@doc.umc.edu.dz

### Аннотация

**Введение:** Алжир пережил множество разрушительных землетрясений, приведших к значительным человеческим жертвам, разрушениям зданий и оборудования. **Цель данного исследования** — количественная оценка потенциального ущерба существующих стратегических зданий в городе Константина, расположенном на северо-востоке Алжира, с тем чтобы минимизировать сейсмический риск. Многие из этих зданий — старые, спроектированы и построены в колониальную эпоху, до введения в действие алжирских сейсмических норм. Поэтому их необходимо укрепить и модернизировать.

**Методы:** Для построения кривых хрупкости используется метод LM2, определенный в RISK-UE (WP4), который основан на нелинейном статическом анализе и спектральном отклике. В этом контексте конструктивная система состоит в основном из жестких железобетонных каркасов с неполным стеновым заполнением. В данном исследовании рассматриваются три типа стратегических зданий: малоэтажные (два этажа), среднеэтажные (четыре этажа) и высотные (шесть этажей). Для оценки сейсмических требований используются действующие алжирские сейсмические нормы (RPA99 версии 2003 года). **В результате** построены кривые прочности для двух основных направлений, локального и глобального поведения, которые определяются в соответствии с ограничениями, указанными в FEMA 356/273 и ATC 40. На основе этих результатов построены кривые хрупкости, определяющие четыре состояния разрушения: незначительное, умеренное, обширное и полное с точки зрения спектрального перемещения.

**Ключевые слова:** кривые хрупкости; состояние разрушения; метод LM2; нелинейный статический анализ; железобетонное здание.